Separation of Vortex Shedding Tones and Broadband Signals using SPOD of uPSP Measurements in NASA Ames Wind Tunnel Test

Jie Li[1], E. Lara Lash[2], Kenneth R. Lyons[2], David D. Murakami[2],
Nettie H. Roozeboom[2], Marc A. Shaw-Lecerf[2]

[1]Metis Technology Solutions, Inc.
Moffett Field, CA 94035

[2] NASA Ames Research Center
Moffett Field, CA 94035

Notice to Readers

Certain features and characteristics of the Space Launch System (SLS) vehicle are defined by the U.S. Government as Export-Controlled, Controlled Unclassified Information (CUI). To comply with CUI restrictions, values in some plots and figures have been either removed or normalized to arbitrary values. It is the opinion of the authors that these alternations do not detract from the relevant technical discussions.

Extended Abstract

This paper discusses separation of the vortex shedding tones and the broadband signals using Spectral Proper Orthogonal Decomposition (SPOD) of the Unsteady Pressure-Sensitive Paint (uPSP) measurements in a NASA Ames wind tunnel test.

The uPSP measurements were collected using Innovative Scientific Solutions, Inc. (ISSI) Porous, Fast-Response Pressure-Sensitive Paint (FP-XXX) [1], 40 ISSI four-inch air-cooled Light-Emitting Diodes (LEDs), and 8 Phantom v2512 high-speed cameras at 10,000 frames per second in the test of the Space Launch System (SLS) Block 1 crew vehicle in the 11-by 11-foot transonic test section of the Unitary Plan Wind Tunnel (UPWT) at NASA Ames Research Center in April 2025. Since the processing of the uPSP data of recent SLS test is still on going, the SPOD outputs of the uPSP measurements in a supersonic test at Mach number 1.40 of the SLS Ascent Transient Aerodynamics Test (ATAT) in September 2019 [2, 3] are presented as examples in this extended abstract. The SPOD outputs of the uPSP measurements of the SLS test in April 2025 will be presented in the full paper.

Figure 1 shows the scale model of the SLS Block 1 cargo vehicle in the ATAT installed in the wind tunnel with uPSP applied to the model surface. Figure 2 shows a mode of Dynamic Mode Decomposition (DMD) of the uPSP measurements in the supersonic test at Mach number 1.40 of the SLS ATAT at a specific frequency, visualized on the surface of the scale model. Figures 3(a) and 3(b) show the magnitude and phase of the DMD mode at the same frequency, respectively, plotted on the plane of x-coordinate and azimuth angle of the nodes. As shown in Figs. 2 and 3, the vortex shedding tones, generated by the forward attachment of the Solid Rocket Boosters (SRBs), are observed in the DMD mode at the frequency [4, 5].

SPOD [6-8] is derived from a space-time proper orthogonal decomposition problem for statistically stationary flows. SPOD modes are determined in the frequency domain. Each SPOD mode oscillates at a single frequency. In a previous paper, the SPOD outputs of the uPSP measurements are presented and the effectiveness of SPOD in the identification, diagnosis and analysis of the aerodynamic and aeroacoustic phenomena is demonstrated [9]. In this paper, it is demonstrated the vortex shedding tones can be effectively separated from the broadband signals in the time domain with the Inverse SPOD of the dominant SPOD modes of the uPSP measurements.

The uPSP measurements on 1,248 selected grid nodes on the SLS center body were used to generate the SPOD outputs. The timeseries of 96,256 frames of uPSP measurements were partitioned into 94 non-overlapping blocks and

a rectangular window was applied in the Discrete Fourier Transform (DFT) of 1,024 frames of uPSP measurements in each block. In Fig. 4, the grid nodes of the SLS center body are illustrated as black dots on the plane of x-coordinate and azimuth angle of the nodes and the 1,248 selected grid nodes are illustrated as red dots. Figure 5 shows the energy (unit: psi^2, in logarithmic scale) of all SPOD modes of the uPSP measurements on the selected grid nodes in the supersonic test at Mach number 1.40 of the SLS ATAT as the function of frequency (unit: Hz, in linear scale). Three peaks are observed in the energy of the 1st SPOD mode, corresponding to the vortex shedding 1st, 2nd and 3rd harmonics. The 1st SPOD mode occupies 99.2%, 89.6% and 49.8% of the energy of all SPOD modes at the frequencies of the vortex shedding 1st, 2nd and 3rd harmonics, respectively, and occupies 62.3% of the energy of all SPOD modes in the full frequency band.

Let n denote the number of selected grid nodes. Based on the Inverse SPOD, the SPOD mode at a frequency, given by an $n \times 1$ complex vector in the frequency domain, corresponds to a set of n sinusoidal signals oscillating at the frequency in the time domain. Therefore, a set of timeseries of vortex shedding tones can be generated as the sum of m sets of n sinusoidal signals corresponding to the 1st SPOD mode, which is dominant in the supersonic test at Mach number 1.40 of the SLS ATAT, at frequencies in the interested frequency band, where m is the number of frequencies in the band. The set of timeseries of broadband signals is computed as the difference of the set of timeseries of original uPSP measurements and the set of timeseries of vortex shedding tones. Figures 6(a) and 6(b) show the energy (unit: psi^2, in logarithmic scale) of the SPOD modes of two sets of timeseries of vortex shedding tones and broadband signals, respectively, separated from original uPSP measurements on the selected grid nodes in the supersonic test at Mach number 1.40 of the SLS ATAT as the function of frequency (unit: Hz, in linear scale).

The timeseries of average pressures were generated from three sets of timeseries of original uPSP measurements, vortex shedding tones and broadband signals on 144 patches for the structural dynamics analysis of the SLS launch vehicle. As shown in Fig. 4, the 144 patches are grouped in six columns. Azimuth angles are constant for patches in a column. The azimuth angle is 35º, 46 º, 57 º, 123º, 134º and 145º, respectively, for the patches in six columns. The dimension of patches in the direction along the streamline is about 1/6 wavelength of the vortex shedding 1st harmonic. Figures 7(a1), 7(a2) and 7(a3) show the timeseries of average pressures (unit: psi) on a reference patch, shown in Fig. 4, generated from three sets of timeseries of original uPSP measurements, vortex shedding tones and broadband signals, respectively. Figures 7(b1), 7(b2) and 7(b3) show the corresponding Power Spectral Density (PSD, unit: psi^2/Hz, in logarithmic scale) as the function of the frequency (unit: Hz, in linear scale). Figure 8 shows the spectrogram of average pressures on the 144 patches. In each plot of the spectrogram, the horizontal axis shows the x-coordinates of the patches, and the vertical axis shows the frequency. The spectrograms generated from three sets of timeseries of original uPSP measurements, vortex shedding tones and broadband signals are shown in the 1st, 2nd and 3rd columns, respectively.

The outputs shown in Figs. 6-8 demonstrate the original uPSP measurements are effectively separated into two parts — vortex shedding tones and broadband signals. In addition to the structural dynamics analysis, the separated vortex shedding tones and broadband signals can also be used in the diagnosis and analysis of the aerodynamic and aeroacoustic phenomena of the pressure field on the surface of the SLS launch vehicle. For example, the broadband signals, with the vortex shedding tones removed, can be used in the extraction of parameters of the Corcos model in the estimation of the Buffet Forcing Functions (BFFs) of the SLS launch vehicle [10].

The work described in this paper is a part of NASA's development of a new state-of-the-art uPSP capability in production wind tunnels. Funding was provided by the NASA Aerosciences Evaluation and Test Capabilities (AETC) Project. The software used to generate the SPOD outputs and the timeseries of vortex shedding tones and broadband signal makes use of the open-source packages *SPOD* [7, 11] in MATLAB and *PySPOD* [12] in Python.

References

[1] Innovative Scientific Solutions, Inc., Porous, Fast-Response Pressure Sensitive Paint Data Sheet. https://innssi.com/wp-content/uploads/Pressure_Sensitive_Paint/Porous_Fast_PSP/Documentation/Porous-Fast-Response-PSP-FP-XXX-Data-Sheet.pdf. Accessed: 13 May 2025.

[2] Roozeboom, N. H., Murakami, D. D., Li, J., Powell, J. M., Baerny, J. K., Stremel, P. M., Volden, T. R., Flach, R. L., Douthitt, A. N., Steva, T. B., Ross, J. C., and Bell, J. H., "Recent Developments in NASA's Unsteady Pressure-Sensitive Paint Capability", AIAA Paper 2020-0516, AIAA SciTech Forum, Orlando, FL, January 2020.

[3] Roozeboom, N., Murakami, D., Li, J., Shaw-Lecerf, M., Lash, E.L, Califano, N., Stremel, P., Lyons, K., Baerny, J., Barreras, C., Ortega, J., Kato, K., Hand, L. and McLachlan, B., "NASA's Unsteady Pressure-Sensitive Paint Research and Operational Capability Developments", AIAA Paper 2023-0636, AIAA SciTech Forum, National Harbor, MD & Virtual, January 2023.
[4] Li, J., Lash, E. L., Roozeboom, N. H., Garbeff, T. J., Henze, C. E., Murakami, D. D., Smith, N. T., Baerny, J. K., Hand, L. A., Shaw-Lecerf, M. A., Stremel, P. M., and Tang, L. Z., "Dynamic Mode Decomposition of Unsteady Pressure-Sensitive Paint Measurements for the NASA Unitary Plan Wind Tunnel Tests", AIAA Paper 2022-0141, AIAA SciTech Forum, San Diego, CA & Virtual, January 2022.
[5] Li, J., Roozeboom, N. H., Lash, E. L., Shaw-Lecerf, M. A., Baerny, J. K., Garbeff, T. J., Hand, L. A., Henze, C. E., Murakami, D. D., and Smith, N. T., "Aeroacoustic Analysis using Dynamic Mode Decomposition of Unsteady Pressure-Sensitive Paint Measurements", AIAA Paper 2024-0882, AIAA SciTech Forum, Orlando, FL, January 2024.
[6] Towne, A., Schmidt, O. T. and Colonius, T., "Spectral Proper Orthogonal Decomposition and Its Relationship to Dynamic Mode Decomposition and Resolvent Analysis", *Journal of Fluid Mechanics*, Vol. 847, pp. 821-867, 2018.
[7] Schmidt, O. T. and Colonius, T., "Guide to Spectral Proper Orthogonal Decomposition", *AIAA Journal*, Vol. 58, No. 3, pp. 1023-1033, 2020.
[8] Nekkanti, A. and Schmidt, O. T., Frequency-Time Analysis, Low-Rank Reconstruction and Denoising of Turbulent Flows using SPOD", *Journal of Fluid Mechanics*, Vol. 926, A26, 2021.
[9] Li, J., Lash, E. L., Lyons, K. R., Roozeboom, N. H., Shaw-Lecerf, M. A., Murakami, D. D., and Califano, N. W. W., "Spectral Proper Orthogonal Decomposition of Unsteady Pressure-Sensitive Paint Measurements in Recent NASA Ames Wind Tunnel Test", AIAA Paper 2025-0234, AIAA SciTech Forum, Orlando, FL, January 2025.
[10] Soranna, F., Heaney, P. S., Sekula, M. K., Piatak, D. J., and Ramey, J. M., "Space Launch System Unsteady Forces Developed from Unsteady-Pressure-Sensitive-Paint-based Corcos Model Parameters", *Journal of Spacecraft and Rockets*, Vol. 61, No. 2, March-April 2024.
[11] MATLAB Documentation: spod. https://www.mathworks.com/matlabcentral/fileexchange/65683-spectral-proper-orthogonal-decomposition-spod. Accessed: 26 March 2024.
[12] Mengaldo, G. and Maulik, R., "PySPOD: A Python package for Spectral Proper Orthogonal Decomposition (SPOD)", *Journal of Open Source Software*, 6(60), 2862, 2021.

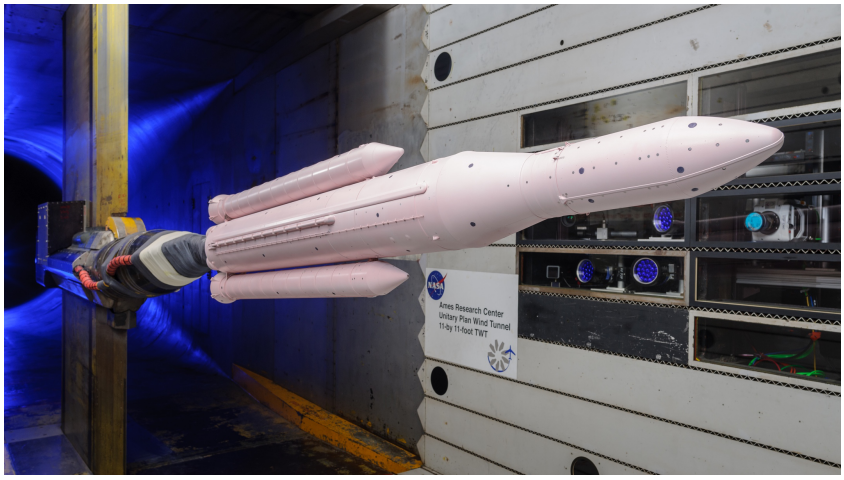

Figure 1 Scale model of the SLS Block 1 cargo vehicle with uPSP in the 11-by-11-foot transonic test section of the UPWT at NASA Ames Research Center during the ATAT in September 2019.

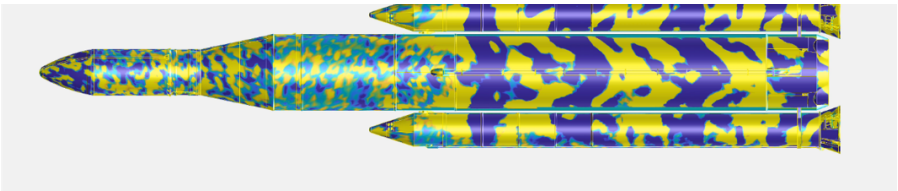

Figure 2 DMD mode of the uPSP measurements at the vortex shedding frequency in the supersonic test at Mach number 1.40 of the SLS ATAT, visualized on the surface of the scale model.

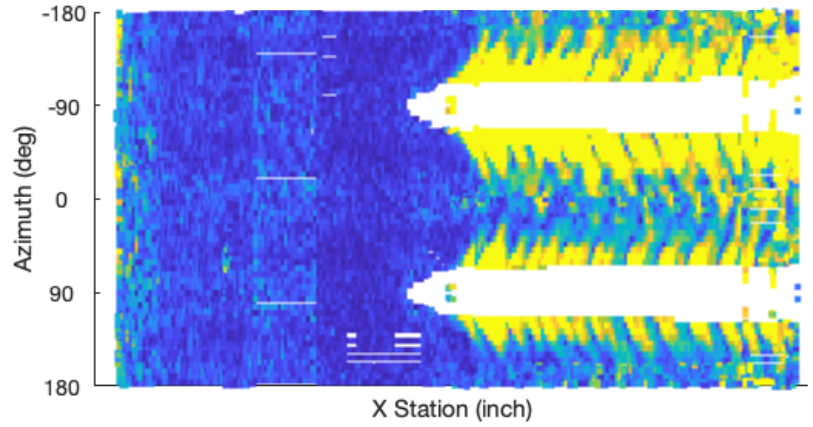

(a)

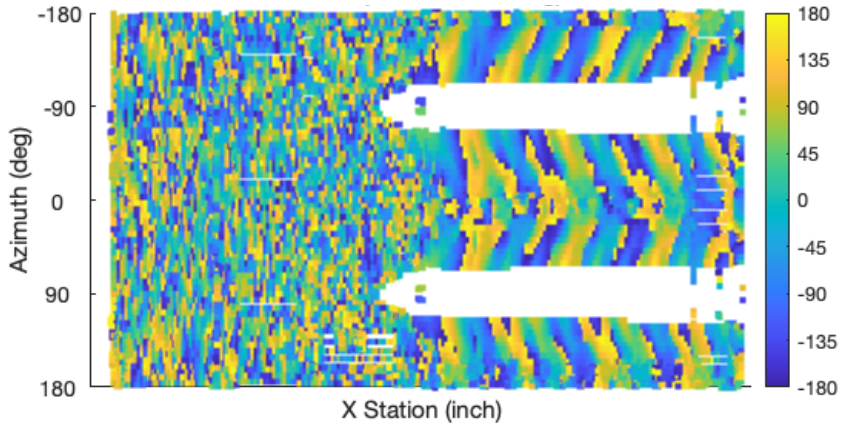

(b)

Figure 3 Magnitude (a) and phase (b) of the DMD mode of the uPSP measurements at the vortex shedding frequency in the supersonic test at Mach number 1.40 of the SLS ATAT, plotted on the plane of x-coordinate and azimuth angle of the nodes.

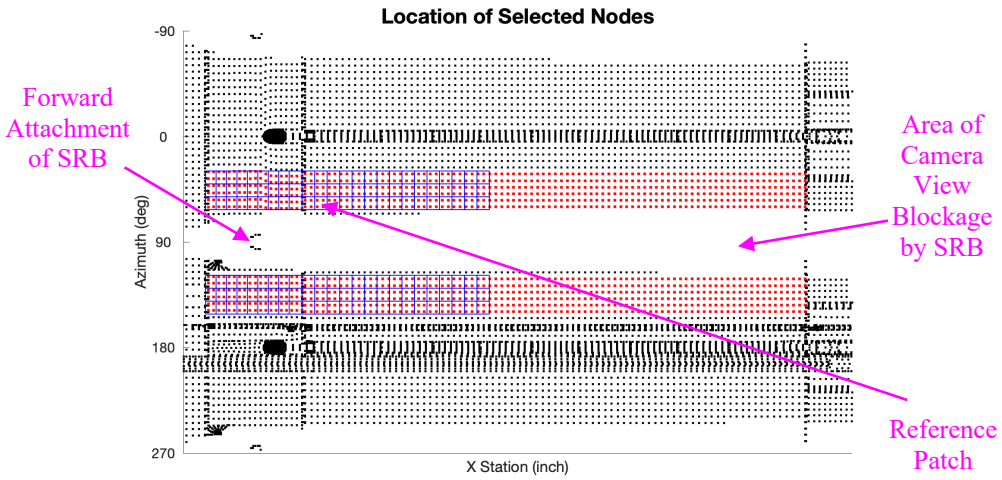

Figure 4 Grid nodes of the SLS center body, plotted on the plane of x-coordinate and azimuth of the nodes. The 1,248 selected grid nodes are illustrated as red dots.

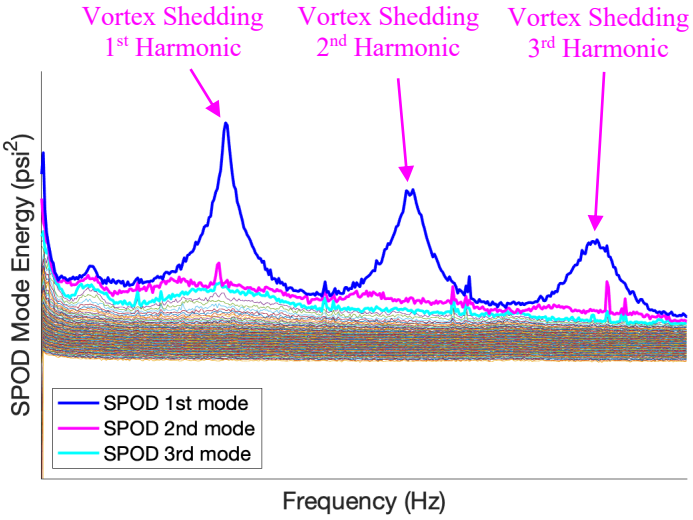

Figure 5 Energy of SPOD modes of the uPSP measurements on the selected grid nodes in the supersonic test at Mach number 1.40 of the SLS ATAT.

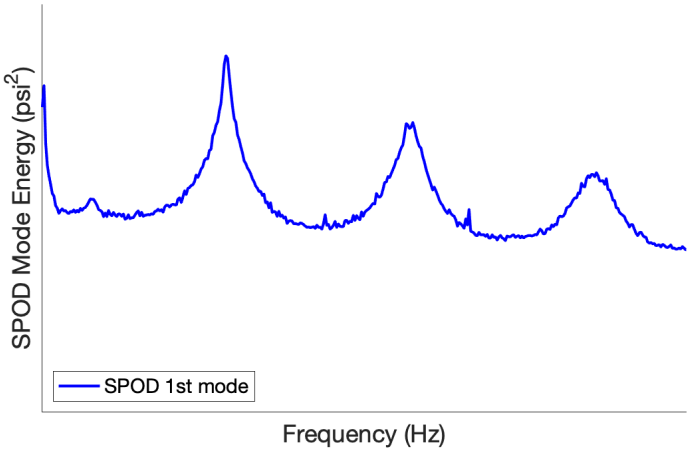

(a)

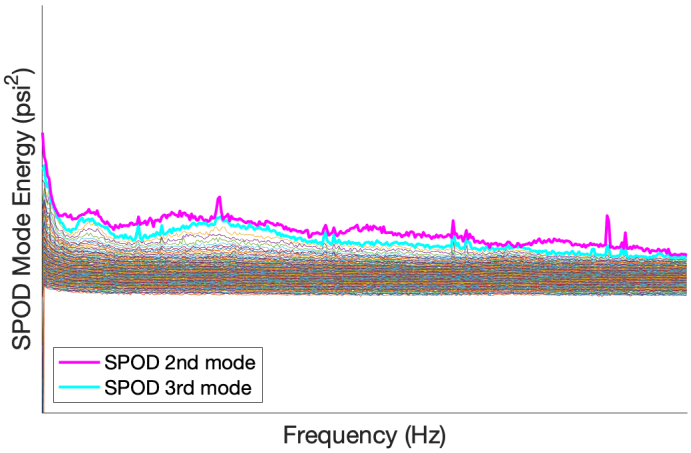

(b)

Figure 6 Energy of SPOD modes of two sets of timeseries of vortex shedding tones (a) and broadband signals (b), separated from original uPSP measurements on the selected grid nodes in the supersonic test at Mach number 1.40 of the SLS ATAT.

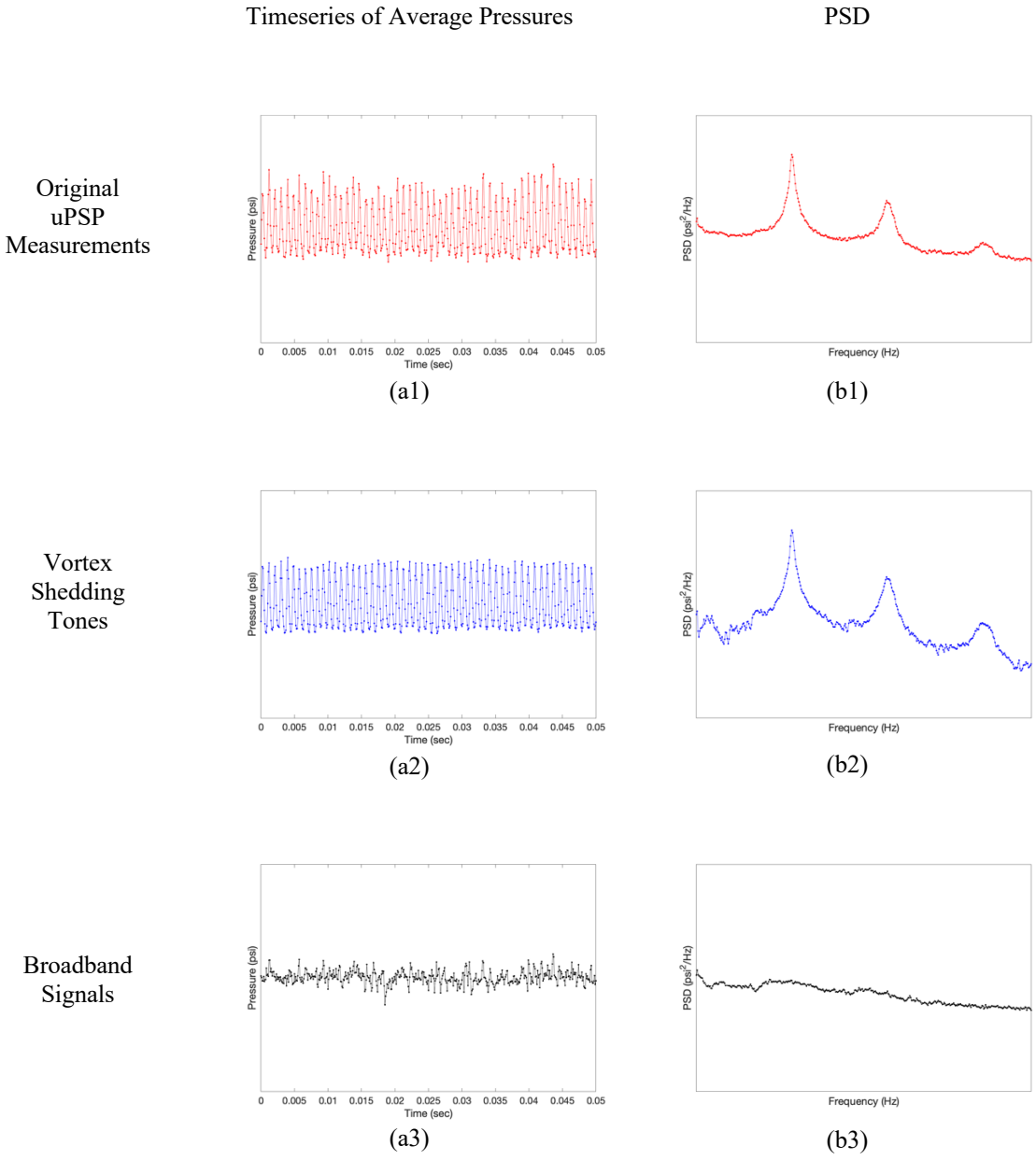

Figure 7 Timeseries of average pressures (a1, a2, a3) on the reference patch and the corresponding PSD (b1, b2, b3), generated from three sets of timeseries of original uPSP measurements (a1, b1), vortex shedding tones (a2, b2) and broadband signals (a3, b3).

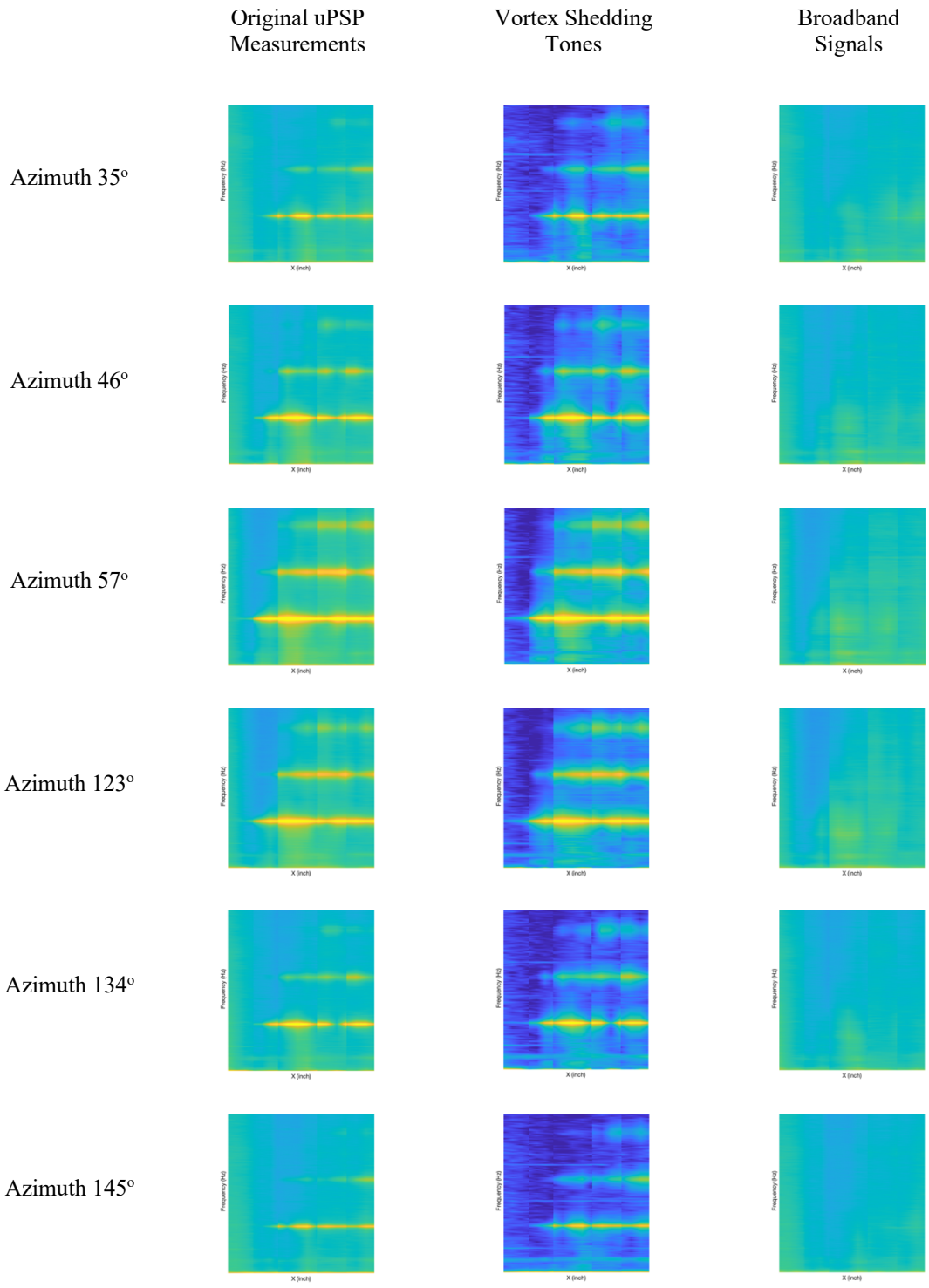

Figure 8 Spectrograms of timeseries of average pressures on 144 patches, generated from three sets of timeseries of original uPSP measurements (1st column), vortex shedding tones (2nd column) and broadband signals (3rd column). Rows 1-6 show the spectrograms of timeseries of average pressures on the patches at azimuth of 35°, 46°, 57°, 123°, 134° and 145°, respectively.